NTNU – Trondheim
Norwegian University of
Science and Technology

Superdirective Microphone Arrays for Real Time Traffic Measurements

Einar Høye Ådnøy

Master of Science in Electronics
Submission date: June 2013
Supervisor: Odd Kr. Pettersen, IET
Co-supervisor: Tonni Franke Johansen, SINTEF

Norwegian University of Science and Technology
Department of Electronics and Telecommunications

Abstract

The measurement of sound power from a car has traditionally been done by taking the car to a test site and driving it past a microphone several times. The use of microphone arrays and beamforming can make the aperture able to single out one car and follow it, taking a measurement of it, while suppressing the sound from the traffic around it. This master thesis studies two algorithms that might be used in this kind of set up: The Delay and Sum (DAS), and the Sparsity Constrained - Deconvolution Approach for the Mapping of Acoustic Sources (SC-DAMAS). This thesis tries to answer the questions: Is SC-DAMAS a better beamforming algorithm than DAS? And are they viable for a real time implementation for the measurement of cars in traffic?

The SC-DAMAS algorithm achieves a far better signal to noise ratio than the DAS. In simulations with background noise levels that are 4 times higher than the source signal, the SC-DAMAS still achieved a signal to noise ratio of 10 dB. SC-DAMAS also excels in low frequency resolution: Where DAS results in a 4 m wide resolution at 400 Hz (for a 2 m long array), the SC-DAMAS manages to pinpoint the source to within one measurement field segment at 200 Hz. DAS on the other hand uses far less resources computing the results from one simulation. The SC-DAMAS used 270 times as much time concluding the simulation compared to DAS. In light of this result it is questionable whether it is possible to implement the SC-DAMAS in a way that lets it measure the sound power levels from a car in real time.

Contents

1 Introduction

To measure the sound power level from a car, the standardized method involves taking the car to a deserted test area to avoid contamination of the measurement from other sources, such as other cars. This is not a very efficient way of characterizing traffic, and can't really be used to identify the amount of noise that come from each car along a road. One of the goals for the SINTEF project for environmental surveillance of traffic, called MOVE, is to measure the sound power level of each individual car in traffic. The use of microphone arrays and beamforming can make the aperture able to single out one car and follow it, measuring it, while suppressing the sound from the traffic around it.

Püschel et al [1] has done the same research for the "Bundesanstalt für Straßenwesen" (Federal Highway Research Institute), and have, according to their article, made a set-up that can accurately measure the sound power of each of the two test cars.

As the MOVE project is in its first year, the focus is mainly on simulation of different algorithms. This master thesis is part of this work and studies the algorithms Delay and Sum (DAS), and the Sparsity Constrained - Deconvolution Approach for the Mapping of Acoustic Sources (SC-DAMAS). Trying to answer the questions: Is SC-DAMAS a better beamforming algorithm than DAS? And are they viable for a real time implementation for the measurement of cars in traffic?

2 Theory

In this chapter some of the basic theory needed to understand the report is shown. Microphone array techniques will be the main focus, starting with the simplest and most robust method Delay and Sum (DAS), then moving on to the more advanced Sparsity Constrained - Deconvolution Approach for the Mapping of Acoustic Sources (SC-DAMAS). At the end some of the problems with microphone array techniques are presented.

2.1 Delay and Sum

The delay and sum (DAS) technique is one of the most basic techniques for beamforming with microphone arrays, and is also the starting point for several other techniques, as described by Yardibi et al [2]. These other techniques seek to combat the drawbacks of the low resolution and high side-lobes that is the weakness of the DAS.

The method can be implemented in both time and frequency domain. In time domain a finite impulse response (FIR) filter is used on each microphone in the array, before the signals are combined (added), as described by Ward et al [3].

The method for frequency domain implementation is based on Yardibi et al [2], an overview of the physical set-up can be seen in figure 1.

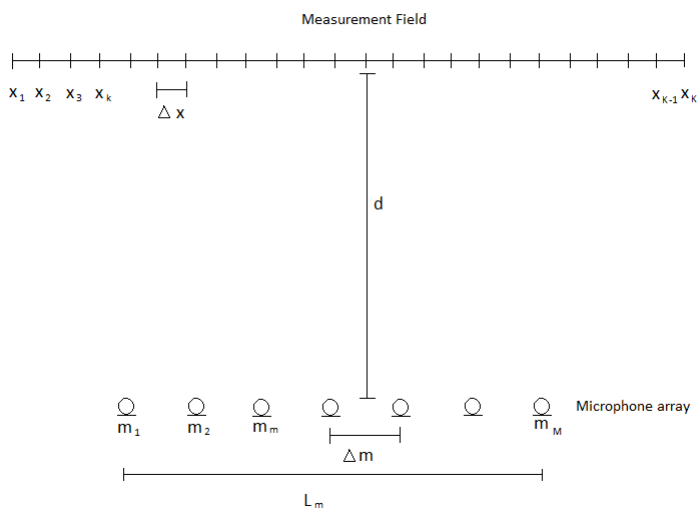

Figure 1: The measurement set-up that is then later processed

The incoming signal from each microphone in an array with M microphones, is divided in I time windows, each 2L long. Then a discrete Fourier transform is done on the time window, converting the data segment into L frequency

bins. The output from a microphone array, in the presence of additive noise, is assumed to be as seen in equation 1:

$$\vec{y}_i(\omega_l) = \vec{A}(\mathbf{x}, \omega_l)\vec{s}_i(\omega_l) + \vec{e}_i(\omega_l) \tag{1}$$

This is the case for each time window $i = 1, ..., I$, and frequency bin $l = 1, ..., L$. The $\vec{A}$ is the propagation matrix defined as $\vec{A}(\mathbf{x}, \omega_l) \triangleq [a(\mathbf{x}_1, \omega_l), a(\mathbf{x}_2, \omega_l), ..., a(\mathbf{x}_K, \omega_l)]$, where $\mathbf{x}_k$ is the source three dimensional position of source $k = 1, ..., K$. $\vec{s}_i(\omega_l)$ is the signal wave form from the sources. It is assumed that the additive noise $\vec{e}_i(\omega_l)$ and $\vec{s}_i(\omega_l)$ are independent zero mean random variables.

The propagation vector for source k is:

$$\vec{a}(\mathbf{x}_k, \omega_l) = \frac{\bar{a}(\mathbf{x}_k, \omega_l)}{C(k,l)} = \frac{1}{C(k,l)} \begin{bmatrix} \frac{1}{x_{1,k}} e^{-j\omega_l x_{1,k}/c_0} \\ \vdots \\ \frac{1}{x_{M,k}} e^{-j\omega_l x_{M,k}/c_0} \end{bmatrix} \tag{2}$$

Where $x_{m,k}$ is the distance between microphone m and source k, and $C(k,l) = ||\bar{a}(\mathbf{x}_K, \omega_l)||_2$, in other words $C(k,l)$ is used to normalize $\vec{A}(\mathbf{x}, \omega_l)$.

To find the source power, the autocorrelation is computed as in equation 3:

$$\hat{R}(\omega_l) = \frac{1}{I} \sum_{i=1}^{I} \vec{y}_i(\omega_l)\vec{y}_i^H(\omega_l) \tag{3}$$

Where $\vec{y}_i^H(\omega_l)$ denotes the conjugate transpose of y. $\tilde{y}_k(\mathbf{x}, \omega_l) = \frac{1}{I}\sum |s_{i,k}(\omega_l)|^2$ is the source power, and can be found as part of the autocorrelation of $\vec{y}_i(\omega_l)$. This leads to the power from a source $\mathbf{x}'$ being as seen in equation 4:

$$\tilde{y}_k(\mathbf{x}', \omega_l) = \frac{1}{M^2}\tilde{a}^H(\mathbf{x}, \omega_l)\hat{R}(\omega_l)\tilde{a}(\mathbf{x}', \omega_l) \tag{4}$$

Where:

$$\tilde{a}(\mathbf{x}_k, \omega_l) = C(k,l) \begin{bmatrix} x_{1,k} e^{-j\omega_l x_{1,k}/c_0} \\ \vdots \\ x_{M,k} e^{-j\omega_l x_{M,k}/c_0} \end{bmatrix} \tag{5}$$

2.2 DAMAS

The SC-DAMAS adds a sparsity constraint to the DAMAS, as such the DAMAS needs explaining before adding the sparsity constraint. This implementation is again based on Yardibi et al [2].

DAMAS tries to improve on DAS by using its results to obtain the deconvolved source strengths. So starting with equation 4 and inserting the equations

3 and 1, we obtain equation 6. As the analysis is done separately for each frequency the ω_l is dropped from the notation for simplicity.

$$\tilde{y}_k(\mathbf{x}') = \frac{1}{M^2}\tilde{a}^H(\mathbf{x}')\left[\vec{A}(\mathbf{x})\left(\frac{1}{I}\sum_{i=1}^{I} s_i s_i^H\right)\vec{A}^H(\mathbf{x}) + \sigma^2 I\right]\tilde{a}(\mathbf{x}') \tag{6}$$

It is then assumed that the cross terms, in equation 6, together with the noise term, can be neglected. The cross terms will be close to zero as long as $I \gg 1$, the noise on the other hand depends on the signal and environment. These assumption then give

$$\tilde{y}_k(\mathbf{x}') = \frac{1}{M^2}\tilde{a}^H(\mathbf{x}')\left[\sum_{k=1}^{K}\frac{1}{I}\sum_{i=1}^{I}|s_{i,k}|^2\vec{a}(\mathbf{x}_k)\vec{a}^H(\mathbf{x}_k)\right]\tilde{a}(\mathbf{x}') = \sum_{k=1}^{K}\tilde{A}_k(\mathbf{x}')\tilde{x}(\mathbf{x}_k) \tag{7}$$

Where

$$\tilde{x}(\mathbf{x}_k) \triangleq \frac{1}{I}\sum_{i=1}^{I}|s_{i,k}|^2 \tag{8}$$

and

$$\tilde{A}_k(\mathbf{x}') = \frac{1}{M^2}|\tilde{a}^H(\mathbf{x}')\vec{a}(\mathbf{x}_k)|^2, \qquad k = 1, ..., K \tag{9}$$

As the number of sources and their placement is unknown we replace K with N scanning points in the measurement region. Naturally $\mathbf{x}$ and $\mathbf{x}'$ is also scanned over the same set of points. The number of points and the distance between these simply depends on the desired minimum spacial accuracy of the application. If the power at each scanning point is stacked up we find that the power vector $\tilde{\mathbf{y}} = \tilde{\mathbf{A}}\tilde{\mathbf{x}}$, each term can be expressed as

$$\tilde{y}_n = \tilde{A}_{n,1}\tilde{x}_1 + \tilde{A}_{n,2}\tilde{x}_2 + \cdots + \tilde{A}_{n,N}\tilde{x}_N \tag{10}$$

The solution for $\tilde{\mathbf{x}}$ can be found by using the Gauss-Seidel method and noting that $\tilde{A}_{n,n} = 1$, resulting in equation 11

$$\tilde{x}_{n^{(k)}} = max\left(0, \tilde{y}_n - \left[\sum_{j=1}^{n-1}\tilde{A}_{n,j}\tilde{x}_j^{(k)} + \sum_{j=n+1}^{N}\tilde{A}_{n,j}\tilde{x}_j^{(k-1)}\right]\right) \tag{11}$$

Here k is the current iteration number limited above by a user defined maximum number of iterations, $\tilde{\mathbf{x}}^0 = 0$ and as $\tilde{\mathbf{x}}$ represents power positivity is ensured.

2.3 Diagonal Removal

The DAMAS algorithm, as described previously, has several drawbacks, one of which is that it neglects the noise term. For a more complete list of drawbacks see Yardibi et al article [2].

The problem with neglecting the noise term in the implementation can be overcome by diagonal removal of $\hat{R}$, in other words setting the diagonal elements of the matrix to zero. In this case the DAS output is calculated as:

$$\tilde{y}^{DR}(\mathbf{x}') = \frac{1}{M^2 - M}\tilde{a}^H(\mathbf{x}')\tilde{R}\tilde{a}(\mathbf{x}') \tag{12}$$

Where $\tilde{R}$ is $\hat{R}$ with the diagonal elements removed. Then, $\tilde{y}^{DR} = \tilde{A}^{DR}\tilde{x}$ where

$$\tilde{A}_k^{DR} = \frac{1}{M^2 - M}\tilde{a}^H(\mathbf{x}')[\vec{a}(\mathbf{x}_k)\vec{a}^H(\mathbf{x}_k)]_{diag.=0}\tilde{a}^H(\mathbf{x}') \tag{13}$$

for each position k=1,...,K. For notational simplicity $\tilde{y}^{DR}$ and $\tilde{A}^{DR}$ will be denoted as $\tilde{y}$ and $\tilde{A}$ from here on.

2.4 Sparsity Constrained DAMAS

As the name suggests, one of the main assumptions made to improve on the DAMAS is that the problem is a sparse problem. As the source positions are unknown, the sources were instead replaced by a measurement field or area, thus the number of points N that are calculated should be larger than the number of sources K. This means that one can assume that $\tilde{x}$ contains a few non zero elements compared to its size. This makes it possible to apply a slightly modified version of LASSO (Least absolute shrinkage and selection operator) to this problem:

$$\begin{aligned} &\text{minimize} \quad \| \tilde{y} - \tilde{A}\tilde{x} \|_2^2, \\ &\text{subject to} \quad \| \tilde{x} \|_1 \leq \lambda, \quad \tilde{x}_n \geq 0, \quad n = 1, ..., N \end{aligned} \tag{14}$$

As $\tilde{x}$ is power every element is forced to be positive. The new quantity λ is here an unknown user parameter, that needs to be empirically found, or calculated based on values of $\tilde{y}$ and $\tilde{A}$. Equation 14 is not very sensitive to the selection of λ, setting $\lambda \to \infty$ reduces the problem to a non-negative least-squares problem. However prior knowledge will improve the estimate in most cases.

In equation 14, λ constrains the l_1 norm of $\tilde{x}$, which represents the total power of the signal. There are several different methods of obtaining the total power of the signal, one of the methods suggested by Yardibi et al [2] starts with the estimate of the covariance matrix. Doing a eigendecomposition on the covariance matrix gives: $\hat{R} = \hat{U}\hat{\Gamma}\hat{U}^H$ where $\hat{\Gamma}$ is a diagonal matrix with the eigenvalues of $\hat{R}$, arranged in nonincreasing order. The user parameter is then determined by:

$$\lambda = Tr(\hat{\Gamma} - \hat{\gamma}_M I) \tag{15}$$

Where $\hat{\gamma}_M$ is the smallest diagonal element of $\hat{R}$ and should consist of the noise effect.

2.5 Constant Directivity Beamforming

Using a microphone array with a set size gives a beam that expands towards lower frequencies. Ward and colleagues [4] suggest that to get a constant beam shape for an arbitrary frequency requires that the total size of the aperture remains constant compared to the wavelength. Also the total aperture should be larger than the wavelength, as the larger the total array is the better the resolution becomes. In the ideal case an aperture with infinite number of sensors is used, and for each frequency a subset is used so that the relationship between wavelength and aperture size remains constant. In practice this is not possible. Instead an array with total size constant compared to the wavelength needs to be made for every frequency bin of interest. The problem with this implementation is that if you want a measurement over a large frequency band, then this will require a lot of microphones. Also at lower frequencies that gives a large total size, 50 Hz gives a wavelength of $6.8m$, making a rig that might be impractical.

2.6 Grating Lobes

One of the problems that occur when using the DAS, and in extension SC-DAMAS, is the occurrence of grating lobes. When delaying the incoming sound at the different microphones most of the sound from other directions than the main lobe will be dampened. If the array is poorly designed then grating lobes will occur due to positive interference between neighbouring array elements. The array response when using a far field assumption is according to Angelsen [5] as seen in equation 16.

$$A(r,\omega) = \frac{e^{ikr}}{2\pi r} M \frac{\sin[kd(\sin\theta - \sin\theta_0)M/2]}{M\sin[kd(\sin\theta - \sin\theta_0)/2]} = M\frac{\sin(\beta M/2)}{M\sin(\beta/2)} \tag{16}$$

Here the $\beta = kd(\sin\theta - \sin\theta_0)$, M is the number of microphones, d the distance between microphones, k is the wave number, θ_0 is the angle of the main lobe, in other words the direction that the array is focusing, and θ is the response angle. The array response will have periodic peaks for $\beta_p = 2\pi p, \quad p = 0, \pm 1, \pm 2, \ldots,$ as $\sin(\beta/2) = 0$. The peak for $p = 0$ is found for $\theta = \theta_0$ and is the main lobe in the steering direction. The other values of p can produce grating lobes, if there exists a value θ which produces such a β_p. The existence of grating lobes is therefore dependent on the value of kd. Equation 17, shows the formula for grating lobes.

$$\sin\theta_p - \sin\theta_0 = p\frac{\lambda}{d} \qquad p = \pm 1, \pm 2, \ldots \tag{17}$$

A requirement for such a p, is that

$$|\sin\theta_0 + p\lambda/d| \leq 1 \tag{18}$$

The limiting factor for grating lobes is the relationship between d and λ. Depending on how far to each side the array will be focusing the conditions to avoid grating lobes increases, table 1 shows a list of these requirements.

θ_{max}[deg]	10	20	30	45	55	65	90
$(d/\lambda)_{max}$	0.85	0.75	0.67	0.59	0.55	0.52	0.5

Table 1: Requirements to avoid grating lobes for various steering angles

3 Method

This chapter describes the work that has been done to investigate the algorithms described above and which values that have been used.

3.1 Implementation

The measurement set-up figure from the theory section is shown again for convenience.

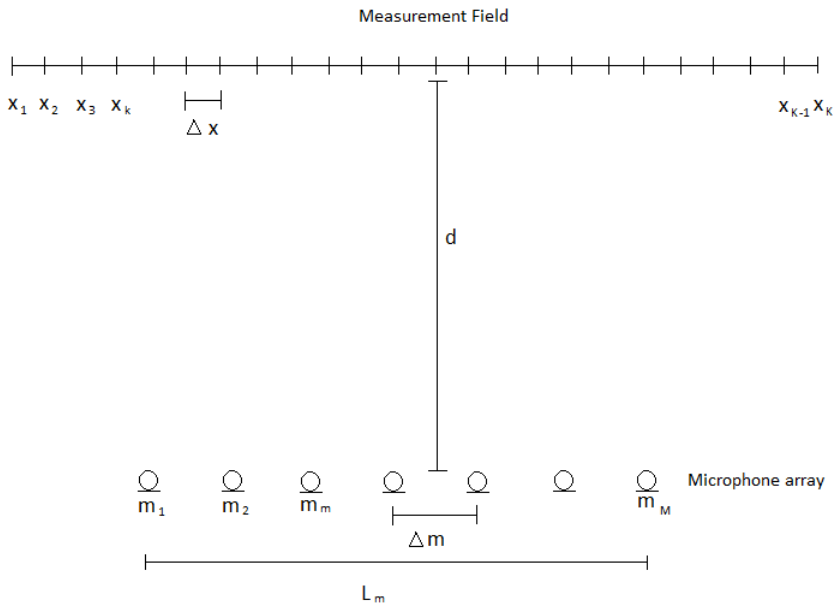

Figure 2: The measurement set-up that is then later processed

The algorithms for DAS and SC-DAMAS were implemented in Matlab, one or more sources were simulated to propagate from point sources localized at some point along the measurement field $X_k, k = 1, ..., K$. The sound effect from each source was attenuated as if the sound was travelling as a plain wave, giving a loss of $\frac{1}{d}$. The sources emit white noise. The total measurement field is $20m$ long positioned from $-10m$ to $10m$, the distance between two measurement positions, Δx, is set to $0.2m$, making a total of 101 points. A background noise field is also simulated as a constant level of white noise at each microphone, the amount of noise can be varied from none to several times that of the signal strength. The noise field measured by one microphone is assumed to be uncorrelated with the other microphones, this simulates noise from the equipment, self noise, and to a certain extent a general background noise field. The microphone array was positioned a distance d from the source

measurement field, d is set to $7m$. The microphones in the array are placed a distance Δm between each other, Δm is not a fixed distance and may even vary along the array, as with an expanding aperture. The total size of the aperture varies from each implementation depending on number of microphones and the distance, Δm, between them, this size is set as L_m. For convenience these numbers have been written in table 2.

Measurement field	$20m, \in [-10m, 10m]$
Δx	$0.2m$
Distance d	$7m$
Δm	Constant or variable
Microphone array L_m	Varies

Table 2: Set-up values

As a standard to compare the rest of the measurement against an array of $L_m = 2m$ is chosen with 11 evenly spaced microphones, $\Delta m = 0.2m$. It is not an ideal array, but gives room for improvement to show how different aspects affect the result.

Of algorithm specific set-up the source is delayed and dampened as it would due to wave propagation. The signal is then split in $0.04s$ windows, or segments, before FFT. The source is white noise with standard deviation 1, so when it is received it is dampened to about 1/7 of its initial value as the distance from the source to the receiver is $7m$. The sampling frequency is 22100 Hz, making it high enough to support simulation up to just above 10 kHz. Each simulation is $0.7s$ long. The speed of sound is set to $340m/s$ for all simulations and calculations.

Equipment used for the simulation was one Acer laptop running on a Intel Pentium T2390 - 1.86 GHz dual core, with 4 GB RAM running windows 7. The laptop in question was 5 years of age and not the most powerful machine. Matlab version R2010a, using functions from the signal processing toolbox and the optimization toolbox.

3.2 Spatial Resolution

The first test of the algorithms is to see how well they are able to differentiate between two sources that are close to each other, or in other words, how close can two sources be and still be detected as two sources? To test this one source is placed in the centre of the measurement field, the other source is moved away until two sources are detected.

3.3 Combating Grating Lobes

As the theory states the main way to avoid grating lobes is to have small enough distance between microphones compared to the wavelength of the signal. The problem is then when one is measuring up to 6000 Hz, that corresponds to a wavelength of $0.057m$. The set-up proposed above gives a maximum measurement angle $\theta_{max} = 55°$, making the relationship $\frac{d}{\lambda} = 0.55$. Making the largest distance between to microphones $0.0311m$. The lowest frequency of interest might be 50 Hz, which has a wavelength of $6.8m$. The total array size then depends on the quality of the measurement desired at the lowest frequency, but should in any case be larger than the lowest wavelength measured. Using a total array of $13.6m$ or two times the smallest wavelength one ends up with 438 microphones. This is a number of microphones that is impractical. But to see the result one simulation is done with a total array size of $L_m = 2m$ and a microphone spacing of $\Delta m = 0.03m$, a total of 67 microphones.

A more practical approach is something like the one described in the "constant directivity beamforming" chapter. Where instead of using the entire microphone array for the entire measurement area, one uses a subset of the array for the highest frequencies and then expand the array as the frequency get lower. The set-up in table 3 follows this idea, but dividing in array sections for each octave band rather than each frequency bin. This set-up uses 23 microphones.

Band [Hz]	(Sub)Array size [m]	Δm [m]	New microphones
>4000	0.12	0.02	$\pm 0.6 \pm 0.4 \pm 0.2 \quad 0$
4000	0.24	0.03	$\pm 0.12 \pm 0.9$
2000	0.48	0.06	$\pm 0.24 \pm 0.18$
1000	0.96	0.12	$\pm 0.48 \pm 0.36$
500	1.92	0.24	$\pm 0.96 \pm 0.72$

Table 3: Set-up for expanding aperture

3.4 Low Frequency Resolution

As the goal of the project is to measure the noise from the cars it is also important to be able to measure low frequencies, as the engine noise is mainly low frequency noise [6], around 50 Hz depending on the engine revolutions per minute. Therefore there are experiments with wider total aperture to see how large the array needs to be to get a result at lower frequencies.

3.5 Background Noise

Noise is a problem for many different applications, and should also be simulated to see how much this effects the measurements. Simulations are done with one source and increasing amounts of noise. This should give a picture of this effects the result. The amount of background noise is compared to the received signal. It is also part of the analysis of the small segment variance testing.

3.6 Small Segment Variation

As the goal is to have a real time application, the ability to get an accurate measurement without taking the average of several time segments is essential. As the car is only in one measurement segment for a very short time, the question arises: What happens when, instead of averaging over a long time segment as the theory suggest, you only use one time segment? Each time segment in the normal analysis is $0.04s$ or $40ms$. Is there then any difference when decreasing the segment size to $0.02s$ or $20ms$. Only one source is used for the simulations. Looking at the octave band results, from the small segment simulations, taking the maximum point and comparing it with the other segments, that would previously make one simulation. Both the position of the maximum point, and the value is compared.

3.7 Performance

There has to be a trade-off with any algorithm, or else there would be no point in having different algorithms. In the optimization that is done in the SC-DAMAS more resources are used. How much more resources does SC-DAMAS require, and is this significant?

It needs to be said that the algorithms used have not been implemented in an ideal way. Then again using Matlab will not be nearly as effective as implementing an algorithm in c++ of similar, so the point of this is mostly to identify whether there is a big difference in the time and resource usage between DAS and SC-DAMAS.

To get an idea of where and how much computer resources is used on the different algorithms, the "profile" function in Matlab is used, giving a detailed view of the different functions and their time usage.

4 Results

In this chapter the results from the simulations will be shown and briefly commented. More comments and a discussion will follow in the discussion chapter.

4.1 First Comparison

First we start with a general comparison of the DAS and SC-DAMAS beamformer results. These results are like a basis to start improving from. In the following sections, one new aspect of the array is changed to see the result while holding the rest constant. This is done in order to have full control over which aspects that are affected by changing one aspect of the array. The first figure, 3, is from a simulation with a total aperture of $2m$, with an equal spacing between microphones of 0.2. The x-axis represents the frequencies, the y-axis the position along the measurement field. The red colour indicates a high energy, whereas dark blue indicates little or none energy. The dynamic area of the colours is 40 dB between dark blue and dark red.

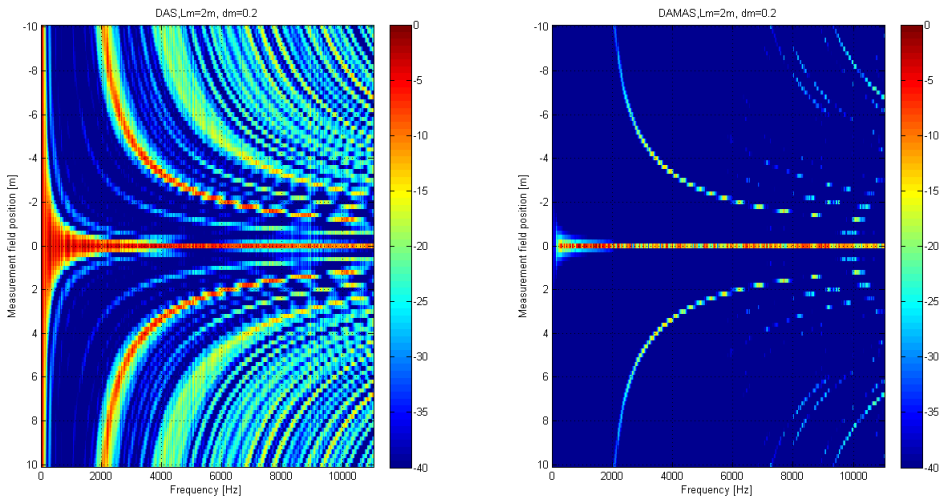

Figure 3: Comparison DAS and SC-DAMAS, $L_m = 2m, \quad \Delta m = 0.2m$

Studying figure 3 we see that both beamformers predict position correctly as the source is placed in x=0. At the same time there are quite strong grating lobes starting around 2000 Hz, especially in the DAS image. These kind of images might be interesting and give a human some understanding of the workings of the beamformer, but for a computer it is hard to interpret. Also as the total power measurement that will be obtained often is A-weighted, dividing the frequencies in octave bands is the first step. It also makes it easier to see

details at lower frequencies. The octave band frequency plots are shown in figure 4, there is no weighting applied to the different octave bands. The reason for the difference in levels of the different octave bands is that the source signal is white noise, and dividing in octave bands doubles the number of frequency bins in each octave band.

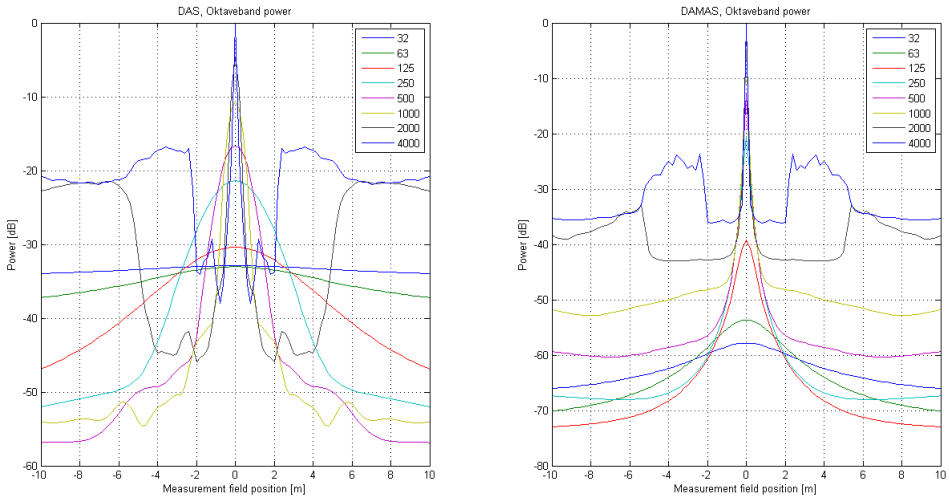

Figure 4: Octave band power representation

Starting with the highest frequencies in figure 4, it is hard to distinguish between the different curves, especially as we approach the source position. The ideal beamformer should have a Dirac like plot for all frequencies, with one top at the source location and nothing all other places. As the results at the higher frequency bands come somewhat close to this the curves coincide making them hard to read, but this is also a sign that the measurement is good. Uniformity is in this respect positive. The lower frequencies on the other hand show large main lobes, making them impractical for source location. Lobe width is found by starting at the maximum value of the lobe, then moving to each side till the level has decreased sufficiently, the physical distance between these two parts of the lobe is then the lobe width. In this paper we use the value -6 dB as the deciding value. With this we can characterize the resolution in each band by its lobe width as seen in table 4.

The first thing that needs explaining from table 4 is the two lowest frequency bands of DAS, the N/A is simply because a 6 dB drop from the maximum level was not achieved within 10 m. The width of 12 m is also quite wide, and as the application should be able to pinpoint the source, this falls short of the criteria. It is also apparent that there is a very precise source location at the highest octave bands with this set-up. The problem with the low frequencies will be the next focus.

Frequency band [Hz]	DAS width [m]	SC-DAMAS width [m]
32	N/A	12
63	N/A	5
125	8	1
250	3.5	0.4
500	2	0.2
1000	1	0.15
2000	0.4	0.1
4000	0.15	0.1

Table 4: Lobe widths. $L_m = 2m, \quad \Delta m = 0.2m$

4.2 Low Frequencies

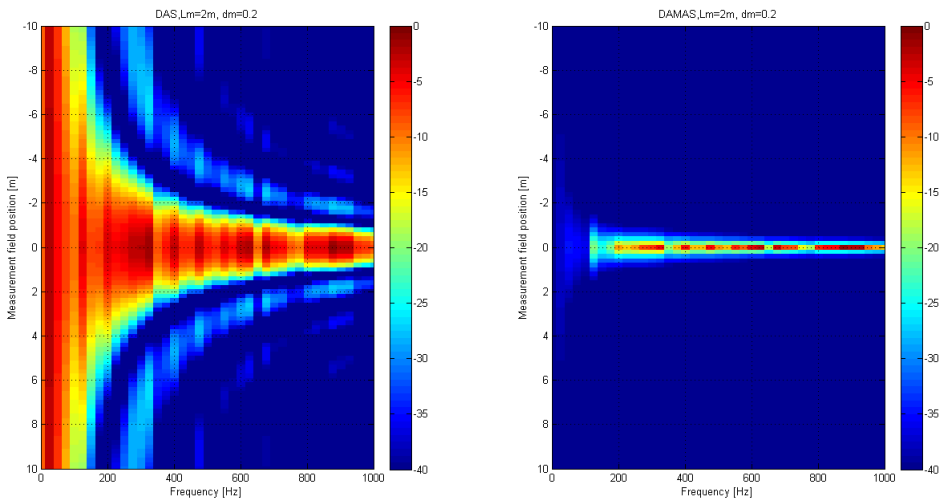

Figure 5: Comparison at low frequencies [0-1000 Hz]

Figure 5 shows the same plots, as in figure 3, but with focus on the frequencies 0-1000 Hz. The SC-DAMAS seems to work ok above 200 Hz, below there is almost nothing. DAS depends on the required resolution, with a 4 m wide source measurement at 400 Hz, and around 3 m wide at 600 Hz. Worth noting is that locating the 6 dB drop is hard or impossible to do accurately in figure 5, so the measured size is an estimate but gives a general idea of the beam width. The wavelength at 200 Hz is 1.7 m, making the lowest frequency measurable (in the SC-DAMAS case), having a wavelength of 1.2 of the total aperture. If the relationship between the lowest frequency and the total aperture size scales linearly then a total aperture size of 8.2 m is needed to get a usable result at 50 Hz. Using an aperture with total size of 8.2 m,

and using an even spacing between each of the 11 microphone ($\Delta m = 0.82m$), results in the figure 6. Using this array and again assuming the scaling property then the 3 m width of DAS should be at around 140 Hz, the 4 m should be at around 100 Hz.

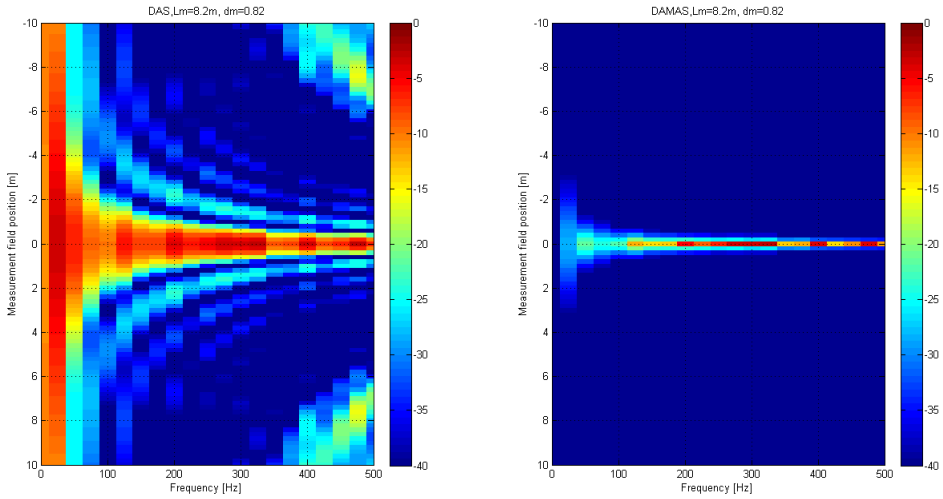

Figure 6: Low frequency test, $L_m = 8.2m$, $\Delta m = 0.82m$, Range [0-500 Hz]

Starting with the DAS of figure 6, we find that the lobe is around 2 m wide at 200 Hz and to compare to the last measurement: 4 m width is now 100 Hz, and at 140 Hz the width is 2.8 m. In the SC-DAMAS case the lowest frequency is around 50 Hz, as one would hope. The same tests have been done with an array of length $L_m = 4.1$ and it seems that the low frequency resolution scales linearly with array size, the result from the 4.1 m test is shown in the appendix in figures 19 and 20.

Converting the results to octave band measurement gives figure 7. Since the focus still is on the low frequencies only the 4 lowest octave bands calculated are shown in the figure. Again starting with DAS, the 32 Hz frequency band seems to be quite a lot flatter than the others, this is due to the wide lobe of the lowest frequencies as seen in figure 6. Figure 7 also gives an indication that the SC-DAMAS works better than DAS at lower frequencies, the fact that the curves are more uniform points to more consistent results. On the other hand the 32 Hz octave band seems to be a bit out of shape, this is understandable as 50 Hz looked to be the lowest frequency with trustworthy result in figure 6. The results are also clearly better when comparing the beam widths as seen in tables 5 and 4. Just the fact that there is a measurable lobe width for the two lowest frequency bands in DAS shows this.

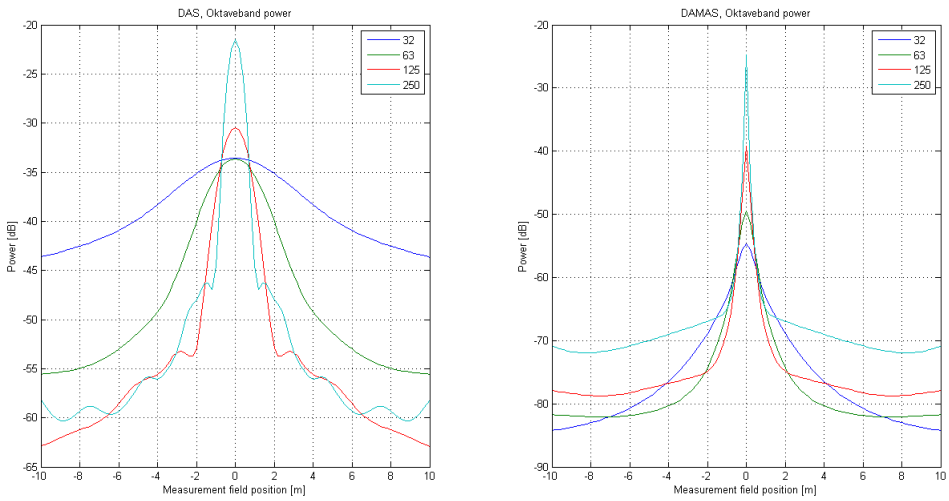

Figure 7: Octave band power representation, $L_m = 8.2m$, $\Delta m = 0.82m$ 32-250 Hz bands

Frequency band [Hz]	**DAS width [m]**	**SC-DAMAS width [m]**
32	10	1.5
63	4	0.8
125	2	0.3
250	1	0.2

Table 5: Lobe widths. $L_m = 8.2m$, $\Delta m = 0.82m$

4.3 Grating Lobes

The simplest implementation with $3cm$ between each microphone in a $2m$ long array gives the results as seen in figure 8.

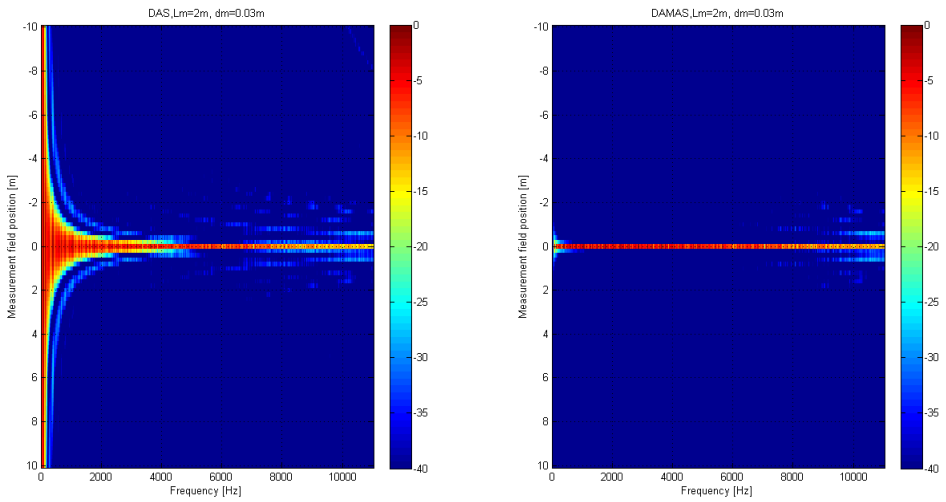

Figure 8: Implementation without grating lobes $L_m = 2m \quad \Delta m = 0.03m$

Using a spacing of $\Delta m = 0.03m$ should remove all grating lobes below 6500 Hz. The result also has good resolution at low frequencies, down to 50 Hz with SC-DAMAS. Being just a 2 m wide array this is a very good result, as the same result needed an array of $8.2m$. There is an absolute downside to the array, and that is the number of microphones. With 67 microphones the rig is impractical, and not very cost efficient.

Following the set up from table 3, the result is seen in figure 9. When comparing the SC-DAMAS of figure 8 with figure 9 we find that the source detection is clearer when using 67 microphones, but other than that the results are very similar. The DAS shows clearly that the measurement aperture is expanding along the frequency range. There also seems to be a general noise level, around 15-30 dB below the source level. This technique does give a large lobe for all frequencies, but on the other hand there are no grating lobes present.

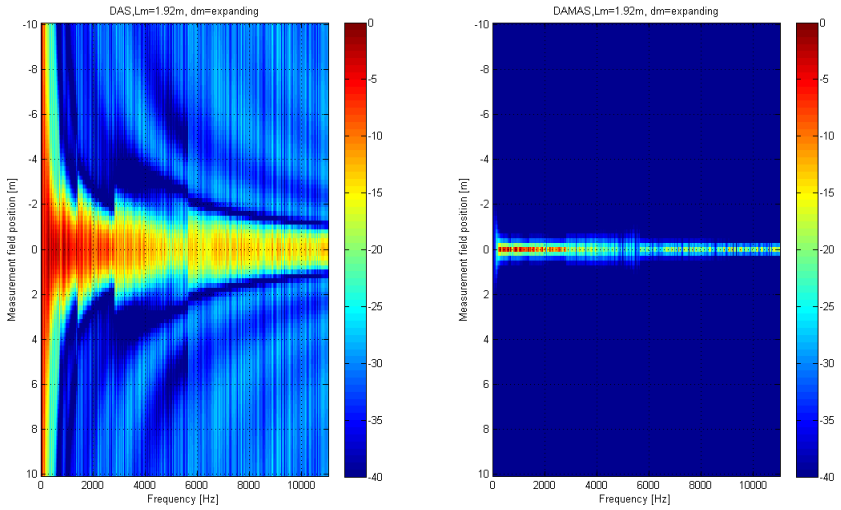

Figure 9: Expanding array to combat grating lobes $L_m = 1.92m \quad \Delta m = expanding$

4.4 Spacial Resolution

One of the fist questions that needs to be answered, is how much of the frequency range that needs to measure two sources for the two sources to be detected. When viewing figure 3 one might assume that above 4-5 kHz it is possible to differentiate between two sources that are 40 cm apart (as the grid step size is 20 cm, 40 cm is the smallest distance between 2 sources before they become 1 large source). Then again at 1 kHz, considerably more space between sources might be needed.

The first part of the analysis is supported by the data in figure 10 and figure 11. Even if almost all of the octave bands only show one source, the 5000 Hz octave band still shows that there are two sources. The sources position have been identified, but the power is not found as all of the lower octave bands are non readable with respect to the different sources.

The second part of the analysis also works when looking at figures 12 and figure 13. As the array is not built for low frequency resolution the lowest bands are having problem with differentiating between the two sources, but it works well from the 500 Hz octave band and above. The 250 Hz octave band almost works in the SC-DAMAS case, and there are clear indications that it is showing two sources. But then again the second source top is not 6 dB above the lowest point between the two sources, and it would not be interpreted as a source.

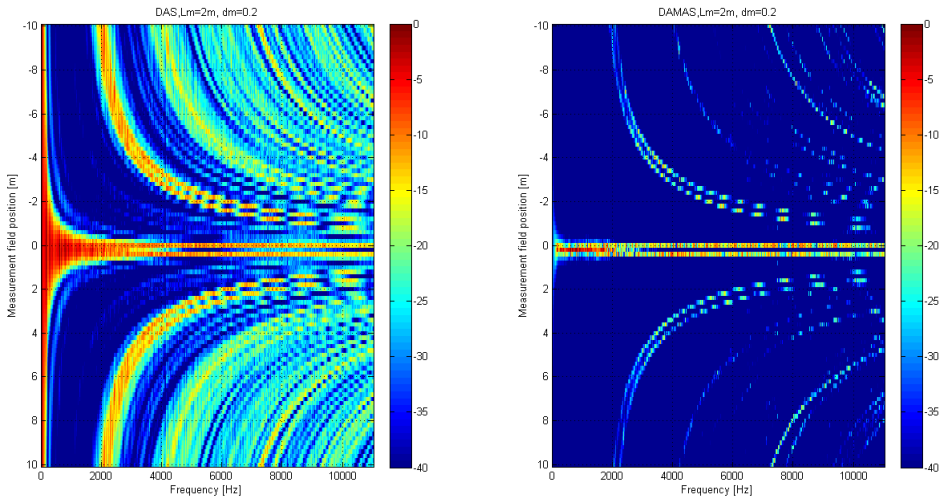

Figure 10: Spacial resolution test, sources 2 segments apart. $L_m = 2m, \quad \Delta m = 0.2m$

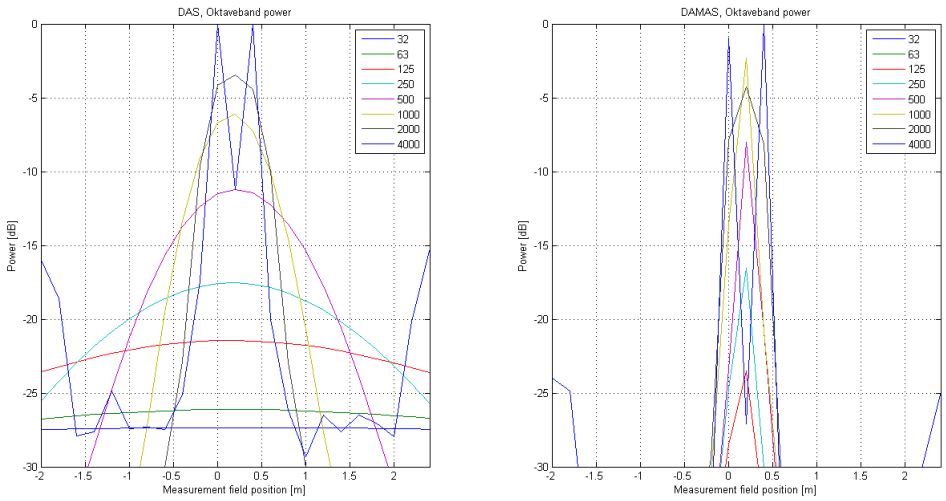

Figure 11: Spacial resolution test, sources 2 segments apart. $L_m = 2m, \quad \Delta m = 0.2m$

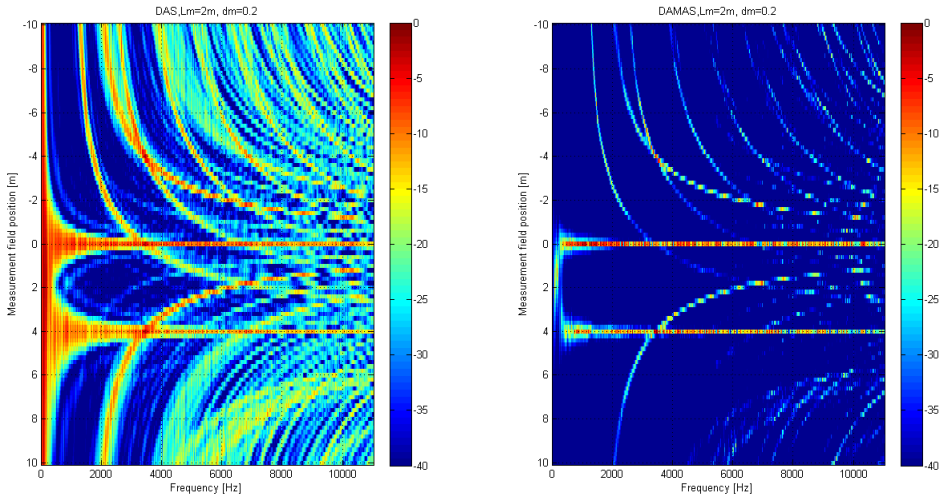

Figure 12: Spacial resolution test, sources 4 m apart. $L_m = 2m, \quad \Delta m = 0.2m$

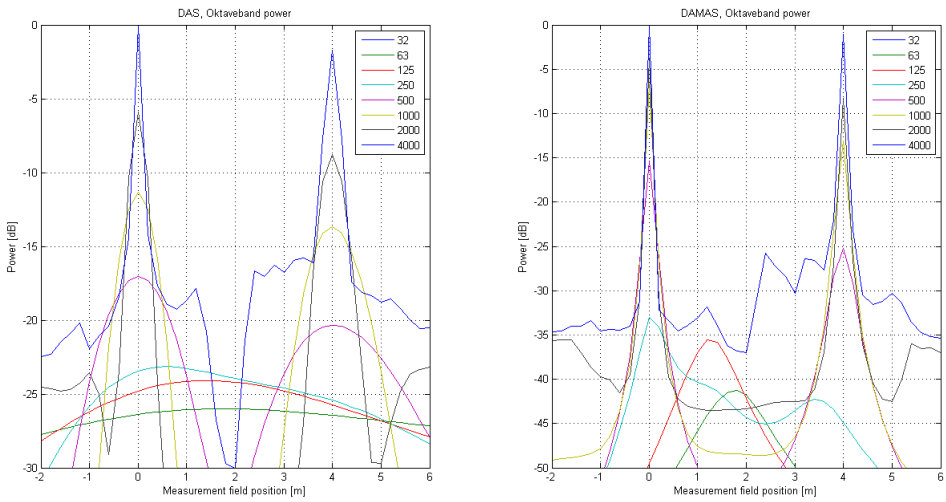

Figure 13: Spacial resolution test, sources 4 m apart. $L_m = 2m, \quad \Delta m = 0.2m$

4.5 Background Noise

Adding noise to the entire microphone array makes it harder to detect the source position. As seen of the figures 14 and 15, the noise level around the signal is higher than in the standard case figures 3 and 4. The noise level around the sources has been increased by 6-10 dB, quite substantial but the DAS estimates still have a SNR of 13 dB, and the SC-DAMAS a SNR of 23 dB. And this is with a general noise level equal to the received source level. The octave band plots are only showing the 125-4000 Hz octave bands as the two lower has poor or no results even without noise added.

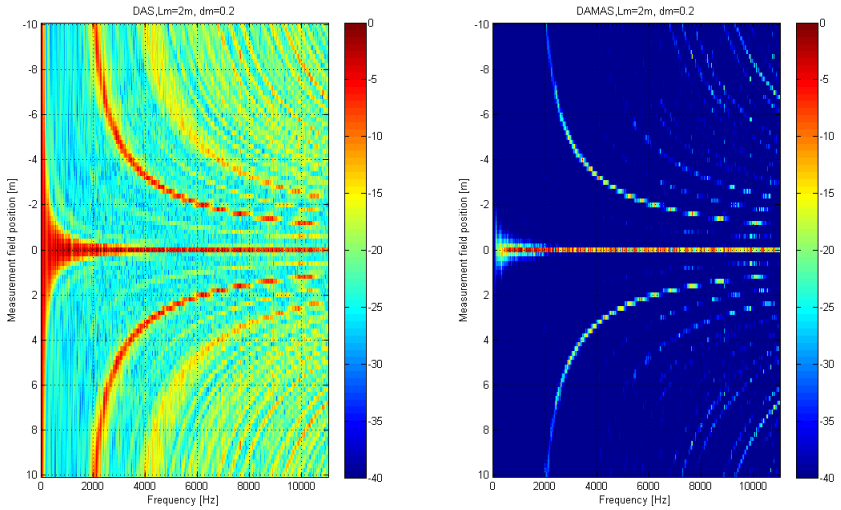

Figure 14: Noise set to equal the signal strength $L_m = 2m, \quad \Delta m = 0.2m$

The algorithms advantage is here that the noise is uncorrelated with each other and the source, and the fact that there is a averaging over several time segments. The algorithms noise suppression is in fact so high that a noise level 3 times as high as the received signal still gives a SNR of 5-6 dB with the DAS, and around 20 dB for SC-DAMAS, thou the low frequency band source detection starts to get affected. See the appendix for these result, figures 21 and 22. The limit for the SC-DAMAS is at 4 times the amount of noise compared to signal. In figure 16 we see that the SNR of the DAS is below 5 dB, the SC-DAMAS on the other hand is still above 10 dB for the highest octave bands, but the low frequency resolution is suffering.

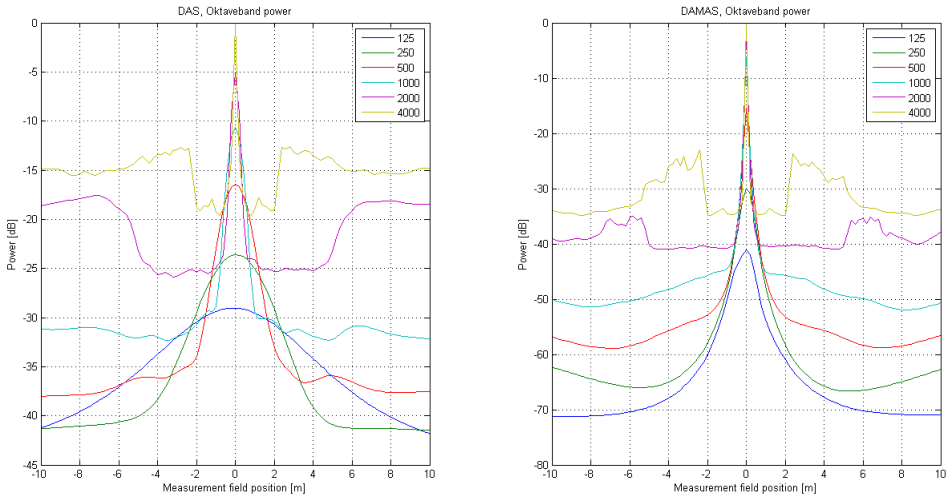

Figure 15: Noise set to equal the signal strength $L_m = 2m, \quad \Delta m = 0.2m$

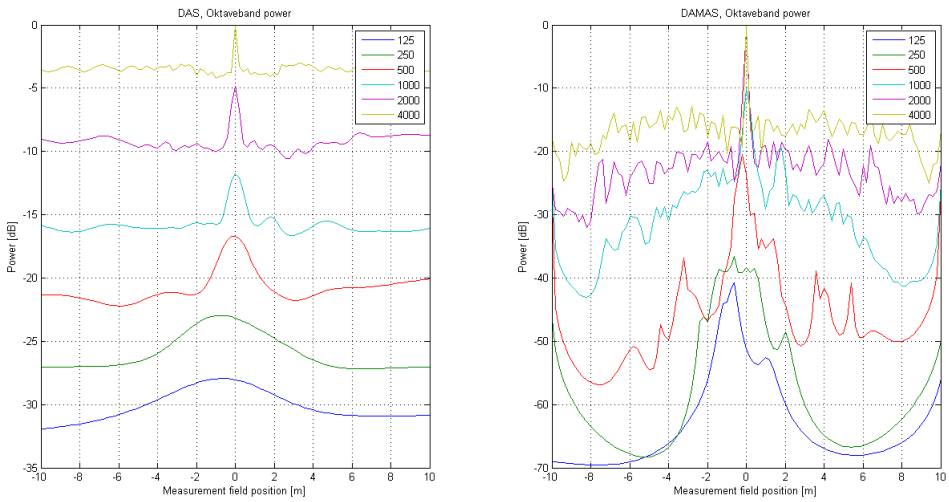

Figure 16: Noise set to 4 times the signal strength $L_m = 2m, \quad \Delta m = 0.2m$

4.6 Small Segment Variation

Figure 17 shows the maximum point of the different octave bands. A total of 15 segments are shown in the figure, the noise level is set to half the signal level. As there are 101 points between $-10m$ and $10m$ in the measurement grid the maximum deviation from the centre is 50 positions, position 0 and 101. The source is placed in position 51. The results from the simulation without noise is shown in the appendix, figure 23.

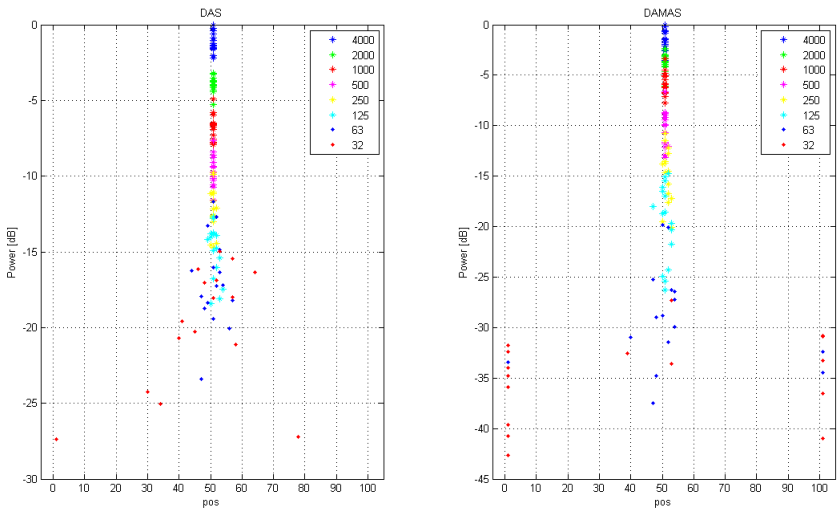

Figure 17: Maximum for each $40ms$ segment and octaveband, noise= $\frac{1}{2} \times signal$

From figure 17 we see that the lower frequencies have a large spread, both in position and in value, this decreases as we come to the higher octave band levels. This can be due to the array being better for octave bands from 250 Hz and above, but might also be due to the increased number of frequency bins in the band which makes them less influenced by randomness in one frequency bin. The total spread, in value, of the 4000 Hz octave band is around $2.5dB$ for both DAS and SC-DAMAS, the spread in value of the 32 Hz frequency band is $12.5dB$, in the DAS case, and around $15dB$ for SC-DAMAS. The spread in measured position is seen in table 6, for both the cases with and without noise. The attentive reader might have noticed that the lower frequencies in SC-DAMAS has a lower octave band power than DAS, this can be explained by the way SC-DAMAS works. SC-DAMAS has an effect limiting factor, which DAS does not have, at the low frequencies the main lobe of the DAS will be very wide with almost full effect everywhere. For SC-DAMAS this then also translates to effect over the entire measurement field, but the effect constraint then makes the level lower.

Table 6 shows the variations that are in position. Δpos is here as in equation

	noise $= 0 \times signal$				**noise** $= \frac{1}{2} \times signal$			
	DAS		**SC-DAMAS**		**DAS**		**SC-DAMAS**	
f [Hz]	$\sum \frac{\Delta pos}{N_{tot}}$	N	$\sum \frac{\Delta pos}{N_{tot}}$	N	$\sum \frac{\Delta pos}{N_{tot}}$	N	$\sum \frac{\Delta pos}{N_{tot}}$	N
32	0	0	0	0	11.56	15	41.63	15
63	0	0	0	0	2.63	12	11.88	15
125	0	0	0	0	0.938	9	1.0	10
250	0	0	0	0	0.312	5	0.813	10
500	0	0	0	0	0	0	0.0625	1
1000	0	0	0	0	0	0	0	0

Table 6: Position deviance for 40 ms segments

19, N is the number of samples that causes this number, in other words, how many segments have their maximum level at another position than the source position (position 51). As the measurement field grid has a spacing of $0.2m$ between each point, a deviation of 1 is the same as miss-calculation of $0.2m$.

$$\Delta Pos = \frac{1}{N_{seg,tot}} \sum_{i=0}^{N_{seg,tot}} |x_i - 51| \tag{19}$$

As can be seen from table 6 the $40ms$ segments without noise has no misses in position, adding noise then makes measurements much less stable, as was also seen in figure 17. Also the deviation from the source position is larger for the SC-DAMAS case. Thou none of the algorithms managed to measure correct position (in any of the segments, with noise) in the 32 Hz octave band, the DAS still had a closer estimate. The SC-DAMAS algorithm has a tendency to collapse measurements to the extreme positions, in the 32 Hz measurement only 3 of the 15 segments are measured to a position that is not 0 or 101, as seen in figure 17. The high amount of misses at the lowest frequency bands is to be expected when looking at former results. With the array used the 32 Hz band gives an almost totally flat response, as seen in figure 4, this makes it easier for small deviations to make big impacts to the measurements.

Decreasing the size of the segments, from $40ms$, to $20ms$ gives figures 18 and 24 (seen in the appendix). As the total length of the signal remains constant the number of segments increases from 15 to 33 (rounding in Matlab gives the reason for more than doubling). The total spread in values has increased with the decreased segment time, the lowest octave band (32 Hz) now has a difference of $20dB$ between the highest and lowest value in the DAS, and around $21dB$ for the SC-DAMAS. The 4000 Hz octave band still seems to have a spread of approximately $2.5dB$ for both algorithms. The reason for the increased spread in the low frequencies might be due to the reduction in time windows (segment size), but it might also be due to the increased number of segments. With more segments, the number of extreme segments should also

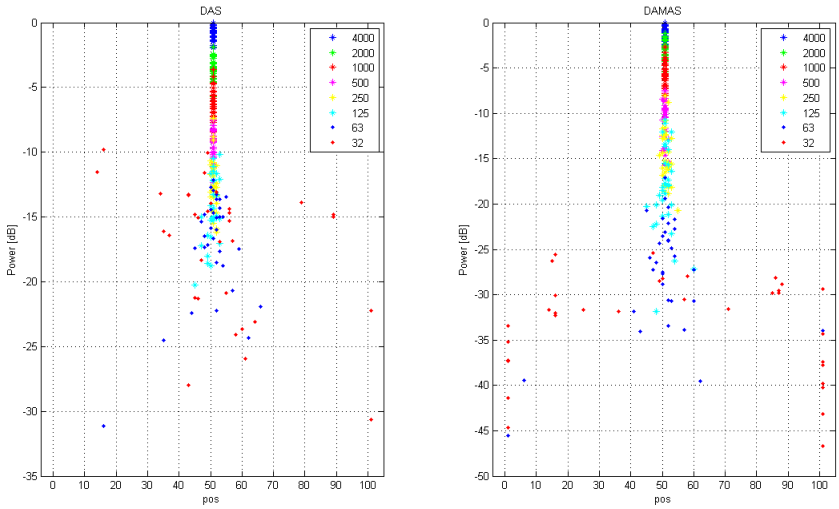

Figure 18: Maximum for each $40ms$ segment and octaveband, noise= $\frac{1}{2} \times signal$

increase, if we assume that random variations are somewhat normal distributed. In other words, the extremes may be larger, but the average and standard deviation may stay the same.

	noise $= 0 \times signal$				**noise** $= \frac{1}{2} \times signal$			
	DAS		**SC-DAMAS**		**DAS**		**SC-DAMAS**	
f [Hz]	Δpos	N	Δpos	N	Δpos	N	Δpos	N
32	1	2	1.0606	1	13.56	33	33.52	33
63	0	0	0	0	4.42	29	7.33	30
125	0	0	0	0	1.15	20	1.606	24
250	0	0	0	0	0.4545	14	0.2121	18
500	0	0	0	0	0	0	0	0
1000	0	0	0	0	0	0	0	0

Table 7: Position deviance for 20 ms segments

Table 7 shows the position results for the $20ms$ segment simulation. The first thing to note is that the simulation without noise no longer has the prefect position prediction that it had in the $40ms$ segment simulation. With noise the story is pretty much the same as with a $40ms$ segmentation. The SC-DAMAS has more and larger deviations, with the exception being the $250Hz$ frequency band where the number is higher, thou the general distance is shorter. The percentage of deviations shows no clear tendency to which has the highest number of deviations when comparing $40ms$ and $20ms$. For DAS the maximum difference is 9% occurring in the 63 Hz octave band ($40ms$ 33%, $20ms$ 42%), the

smallest difference is only 1% occurring in the 125 Hz octave band ($40ms$ 60%, $20ms$ 61%). That being stated, every time there was a difference, the deviation was largest with the $20ms$ DAS simulation, also the average missed distance increases for the $20ms$ simulation compared to the $40ms$. The SC-DAMAS algorithm has different results, with only the 125 Hz frequency band having a higher miss percentage at $20ms$ ($40ms$ 67%, $20ms$ 72%). For all other octave bands the $40ms$ simulations has a higher percentage segments deviating from the source position, the highest difference is again 9% as in the 63 Hz band ($40ms$ 100%, $20ms$ 91%). The average deviation is also largest for the $40ms$ simulation in all bands except the 125 Hz band.

4.7 Performance

The results from the "profile" function in Matlab are shown in table 8. The test is run on the normal set-up with $L_m = 2m, \quad \Delta m = 0.2$, one source and no noise. All results are shown in seconds.

function name	**Calls [n]**	**Total Time**
sc-damas	1	510.25 s
das	1	1.892 s
fmincon	441	502.563 s
createA	1	397.408 s

Table 8: Performance results

As can be seen the SC-DAMAS implementation uses considerably more resources than DAS. The 'fmincon' function is a minimizing optimization function, and is the main part of the SC-DAMAS resource use as can be seen from table 8.

The creation of the A-matrix takes a while and the time increases as the number of microphones and sources increases, as the generation is combining all possible options of sources and receivers. The positive with this is then that the A-matrix, once created can simply be stored and loaded when needed, saving, in this case, almost 400 seconds.

5 Discussion

This chapter discusses the results further, looking at weaknesses and strengths of the results. Starting with the low frequencies, then going on to Grating lobes and noise, the spatial resolution will be discussed as a part of the different topics. At the end the small segment use and the performance of the algorithms is the focus.

5.1 Low Frequencies

Using a total aperture of $8.2m$ it was possible to get results down to 50 Hz using the SC-DAMAS algorithm, thou this result is not as clear as it is at 100 Hz, see figure 6. But there is little doubt that the SC-DAMAS improves well on DAS when it comes to low frequencies. The ability to distinguish between two sources might also be better, or at least clearer. Another problem with achieving good low frequency resolution is the length of the time windows. As the total frequency range is set by the sampling frequency, the size of each frequency bin is decided by the number of samples in the FFT, or in other words, the time slots. At $0.04s$, each frequency bin represents $25Hz$, not just the centre frequency of the bin. When then dividing into octave bands the 32 Hz octave band will then contain only a one or two frequency bins, the 63 Hz octave band 3-5 bins, making them more exposed to random variances that might occur. Also it is common to divide the frequency range not only in octave bands, but $\frac{1}{3}$ octave bands, this would give problems at the lowest frequency bands, as they would cover a smaller frequency range than the frequency bins. According to Nordtest method NT ACOU 109 [7] the frequency range of interest is the $\frac{1}{3}$ octave band starting at 25 Hz and up to 10000 Hz.

Following this the question might be: Why not simply extend the time window? The goal of the project is to measure noise from cars in traffic, in other words moving cars. A car travelling at $80km/h$, or $22m/s$, will travel $0.88m$ in one time segment. The measurement grid has a grid size of $0.2m$, meaning that the car will have moved through four segments in one time slot. Extending the timeslot would only decrease the accuracy of the measurement more, one might in fact, need to shorten the time windows to $0.02s$ or even shorter. A measurement resolution of $0.2m$ might also be unrealistic. With a time window of $0.02s$, the car will travel $0.44m$ in one time frame, a measurement grid with $0.5m$ spacing might then be better.

The use of A-weighting does help the measurement. As the lowest frequencies in any case are being suppressed by the weighting function the result at the lower frequencies is less important. This may allow for a smaller array with less microphones, and still getting a good difference between sources in the A-weighted measurements. Then again the correct A-weighted value should also be composed of correct values at low frequencies. One of the biggest problems

with the lowest frequencies is the spacial resolution. As the main lobe widens at lower frequencies, the ability to distinguish between two sources diminishes. And if there isn't a clear difference between the two sources, a measurement of one might then contain data about the other. Say two cars drive along a road, one car is an electric car, the other is a petrol car. The electric car will produce almost no engine noise, and therefore little low frequency noise, while the petrol car will have a low frequency noise from the engine. If the cars were to drive 4 m apart, and the aperture is 2 m long with 11 evenly spaced microphones, as in figure 12, then the low frequency measurement of the electric car will be dominated by the noise from the engine of the petrol car, as it is stronger, and the beam width is too wide at these frequencies (50-100 Hz).

As the A-weighted level measurements is a sum of the octave band measurements the A-weighted levels might be able to detect two sources in any cases where one octave band shows two sources. As was the case in figure 10. If only looking at the A-weighted levels for two sources that are nearby in space, you can never be quite sure if the measurement is accurate or if most of the lower frequency power is coming from the other source. To avoid this problem one can look at each octave band measurement in addition, or have set limits to how well array separates sources at lower frequencies.

5.2 Grating Lobes

When choosing microphone positions it is possible to eliminate the grating lobes altogether, as seen in figure 8. Removing the grating lobes over a larger frequency range does increase the number of microphones needed. Then again the problem with grating lobes might not need fixing. When studying figure 3, one sees that for the DAS the grating lobe starting around 2000 Hz has approximately the same level as the source measurement, making detecting a true source a problem. For the SC-DAMAS there seems to be a level difference between the source and grating lobe. In this case the grating lobe does not hinder a clear source detection and characterization, it only increases the noise level. Püschel et al [1] uses three different microphone set-ups, with 6, 10 or 20 microphones. The lengths of the arrays were 884, 1375 and 2264 mm. With these apertures the grating lobes will not be eliminated. But as "the microphones were spaced in a way to avoid to have the same distance inside of one array twice", this helps reduce the strength of the grating lobes, as the distance varies more grating lobes will occur, but they will be weaker than the main lobe. This because the grating lobes are generated by the distance between two microphones, which only exists once in the array, thereby being lower than the sum of all the microphones which you get by delaying correctly.

5.3 Background Noise

The fact that it is possible to achieve results with a noise level that is higher than the signal seems too good to be true, but checking the signal shows that it is in fact true. The reason for it working so well is that the noise is uncorrelated with the signal, making it possible to use correlation to our advantage, also the signal is averaged over some time also reducing the impact from uncorrelated noise. The problem in practice is that the background noise might not be completely uncorrelated. Correlated noise might typically be reflections of the car, that therefore have the same characteristics as the cars sound. If the measurement is done along a open highway, there might not be too many reflections, minimizing the correlated noise. Uncorrelated noise sources might typically be noise generated in the equipment, by each microphone, by the amplifiers, and so on, or wind noise. As the algorithms handle this kind of noise well, it might be possible to save some money in buying cheaper equipment, that might generate more noise, and still get satisfactory results.

5.4 Small Segment Variation

As discussed previously, the option of averaging over several time windows is a privilege that we don't have when measuring moving cars. From figures 17 and 18 it seems that the problems that the algorithms had previously are worsened by the small segments and lack of averaging. This is especially the case at lower frequencies. Then again at higher frequencies the maximum values do improve in consistency. This might also be due to the increased number of frequency bins that the octave band consist of, and therefore more results that are added together. One problem that needs discussing is the splitting of the signal in $0.02s$ time windows before FFT. A $50Hz$ sine wave will have one period in $0.02s$, the same as the segmentation time. The FFT is then done on each segment without thought of previous or coming segments, the question is then how well can one decompose into frequency bins when the frequency in question barley has a whole wavelength of information in the FFT, that is if we skip the part where the 50 Hz bin should contain frequency information for more than just 50 Hz. A frequency resolution of 50 Hz (as is the case with $0.02s$ windows) is also questionable if one desires a result at the 32 Hz frequency band, or even if one desires $\frac{1}{3}$-octave band measurement below 200 Hz as the bin size will be the same or larger than the frequency band size.

5.5 Performance

The most processor consuming part of the SC-DAMAS is the minimization with constraints. Yardibi et al [2] propose the use of a Self-Dual Minimization software package, this package was not used in the simulation, instead the

optimization toolbox for Matlab was used with the ”fmincon” function. There might be some advantage to using a more specialized algorithm, but the fact still remains that the minimization requires a considerable amount of iteration, Yardibi et al [2] used 10 000 iterations for one simulation of one frequency. With a segment size of $0.02s$ the number of frequency bins reaches 220 (with a sampling frequency of 22050 Hz). This makes the total number of iterations, for optimizing all frequencies, 2 200 000. If the hope is for a real time application then that number of iterations will have to be done every $0.02s$. The pure numbers of iterations makes for a large trade off. One thing that might help the SC-DAMAS is the fact that multiple core processors are common. As the optimization does not require any result from the other frequencies, the algorithm can easily take advantage of multiple processor cores to reduce the computation time. Another solution might be to stop the optimization before a perfect result is reached, thereby reducing the accuracy of the measurement but at the same time reducing the computation time.

6 Conclusion

Starting with the first question in the introduction: Is SC-DAMAS a better beamforming algorithm than DAS?

It seems that SC-DAMAS has a better signal to noise ratio in its simulation than the DAS, and copes better with increasing background noise levels. The SC-DAMAS simulations managed to achieve a signal to noise ratio of 10 dB with a background noise that was four times higher than the source. The SC-DAMAS also offers a higher suppression of grating lobes, making them less of a problem. The measurement resolution is also increased as the SC-DAMAS tries to reduce the number of sources to the smallest amount possible, this enables octave band measurements at octave bands where DAS would not manage to achieve results. The biggest advantage that DAS has, is efficiency and stability. DAS is a fast algorithm and easy algorithm only using the delay of incoming signals to acquire its result. SC-DAMAS tries to minimize this result, a process that requires thousands of iterations consuming a lot of resources. The SC-DAMAS used 270 times as much time concluding the simulation compared to DAS. The DAS also has the upper hand when dealing with shorter segments and less averaging, making it more stable. Less segments were missing their mark making more stable measurements in the small segment tests.

So to sum up, yes, SC-DAMAS is a superior algorithm when it comes to noise suppression and source resolution, but falls fare short when it comes to speed, and is not as stable as DAS.

Are the algorithms viable for a real time implementation for the measurement of cars in traffic?

The DAS should have no problem in achieving computation times that are faster than the speed at which data arrives at. For SC-DAMAS the problem is bigger. The optimization is time consuming, and might be too consuming to manage to get a real time implementation. One might accept a lower quality result and stop the optimization early, and the question then becomes how few iterations are needed to get a satisfactory result.

As DAS has quite good resolution at the highest frequencies one could use the SC-DAMAS for only a limited part of the frequency range. Then again it is at the lowest frequencies that the SC-DAMAS would most often miss its target in the small segment resolution tests.

One might also accept that SC-DAMAS might not work in real time. Most roads aren't full of cars all the time. If the measurement equipment only turns on when a car is approaching, then is could use the time in between cars to calculate previous measurements, allowing the SC-DAMAS to give results, but not in real time.

There are several parts of the analysis that require more research:

- Finding an optimal optimization algorithm might improve the time used calculating the results from SC-DAMAS.
- Testing the algorithms on real test signals.
- How much of an impact does stopping the optimization earlier have on the SC-DAMAS results?

Acknowledgements

I would like to thank Tony Franke Johannsen for all the guidance he has given me during the work. Also I would like to thank the staff at SINTEF IKT, acoustics department, for input at several stages throughout my work.

7 Bibliography

References

[1] D. Püschel, M. Auerbach and W. Bartolomaeus, *Pass-by Measurements Using Array Techniques*, Euronoise 2009, October

[2] T.Yardibi, J.Li, P.Stoica and L.N. Cattafesta III, *Sparsity Constrained Deconvolution Approaches for Acoustic Source Mapping*, J.Acoust. Soc. Am. 2631-2642, 2008

[3] D. B. Ward, R. A. Kennedy and R. C. Williamson, *FIR Filter Design for Frequency Invariant Beamformers* IEEE Signal Processing Lett., vol. 3, no. 3, pp. 69-71, Mar. 1996

[4] D. B. Ward, R. A. Kennedy and R. C. Williamson, *Constant Directivity Beamforming*, Microphone Arrays - Signal Processing Techniques and Applications, Springer-Verlag, pp 3-17, Germany, 2010

[5] B. A. J. Angelsen *Ultrasound Imaging, Waves, Signals, and Signal Processing, Vol I*, Emantec, pp. 6.21-24, Norway, 2000

[6] S.K.Jha, *Characteristics and Sources of Noise and Vibration and their Control in Motor Cars*, Journal of Sound and Vibration, Volume 47, Issue 4, 22 August 1976, Pages 543-558

[7] Nordtest Methold *NT ACOU 109* Nordtest, Finland, 2001-11

A Appendix - Results

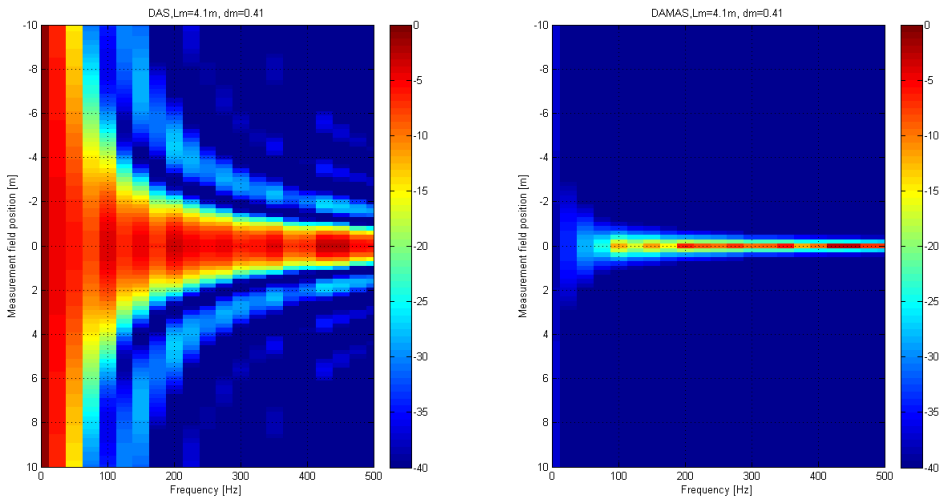

Figure 19: Low frequency test, $L_m = 4.1m$, $\Delta m = 0.41m$, Range [0-500 Hz]

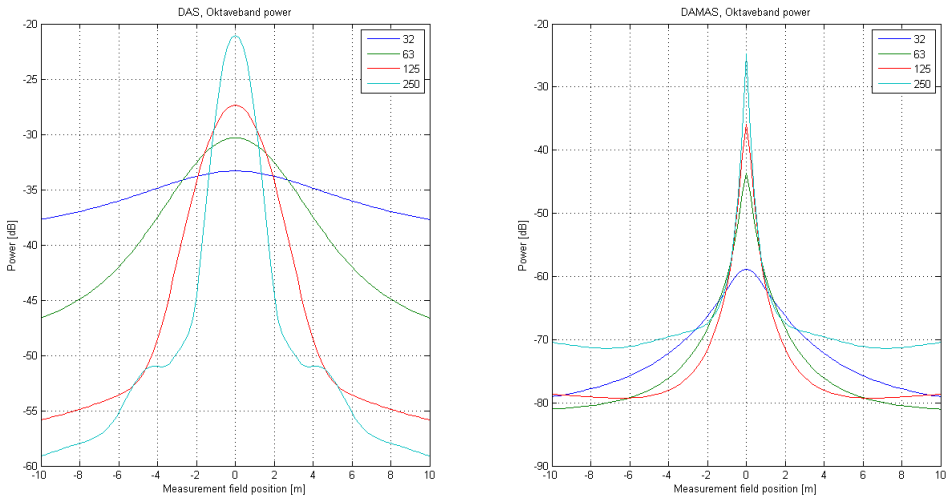

Figure 20: Octave band power representation, $L_m = 4.1m, \quad \Delta m = 0.41m$ 32-250 Hz bands

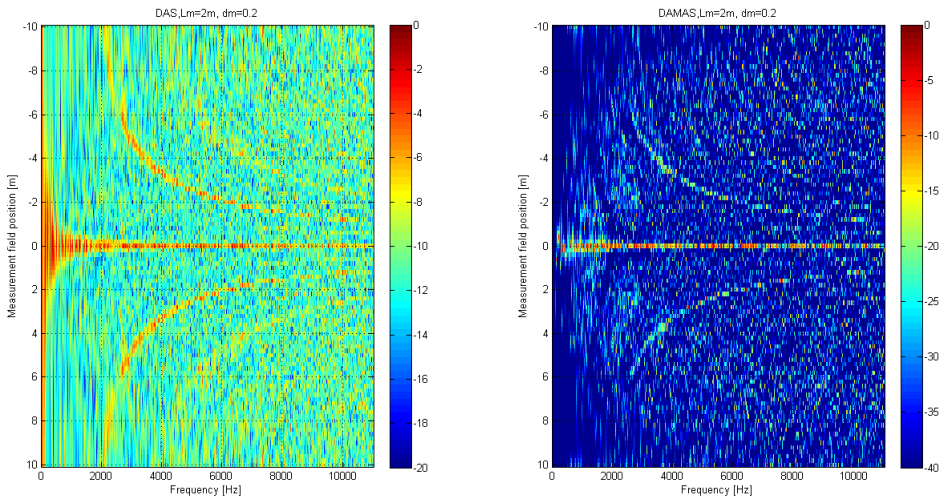

Figure 21: Noise set to 3 times the signal strength $L_m = 2m, \quad \Delta m = 0.2m$

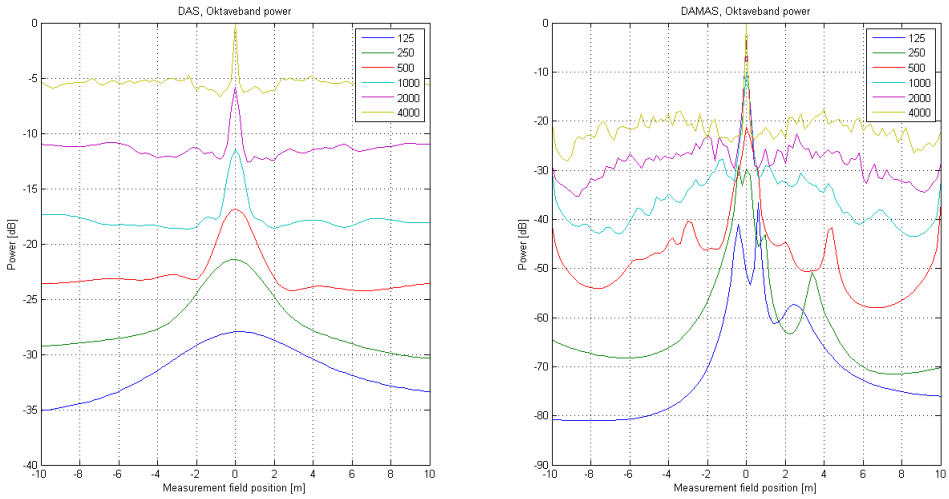

Figure 22: Octave band power, Noise set to 3 times the signal strength $L_m = 2m, \quad \Delta m = 0.2m$

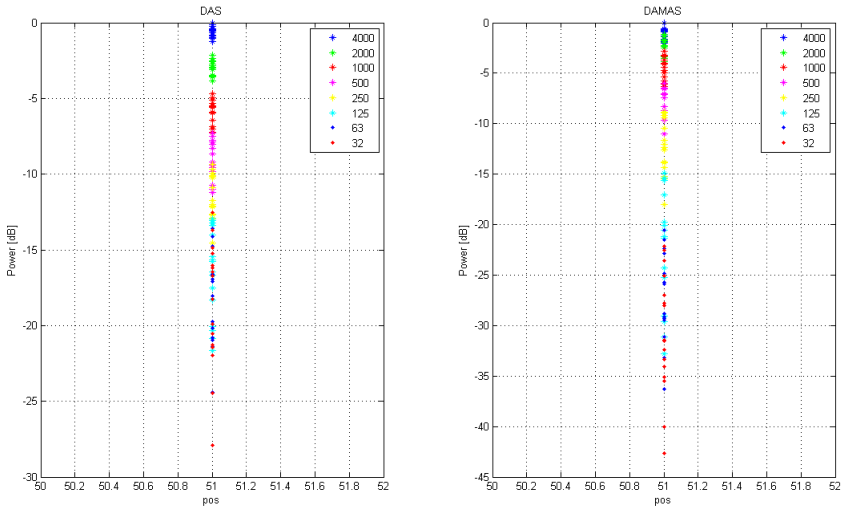

Figure 23: Maximum for each $40ms$ segment and octaveband, no noise

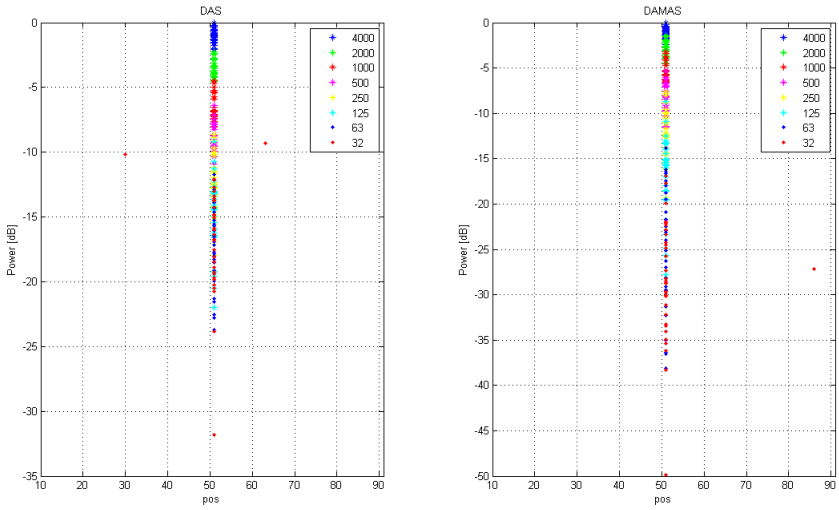

Figure 24: Maximum for each $20ms$ segment and octaveband, no noise

B Glossary

DAS	=	Delay and Sum
DAMAS	=	Deconvolution approach for the mapping of acoustic sources
SC-DAMAS	=	sparsity constrained DAMAS
FFT	=	fast Fourier Transform
L_m	=	Total array size
Δm	=	Distance between neighbouring microphones in array
$\|\| \cdot \|\|_1$	=	l_1 norm: the absolute sum of the elements
$\|\| \cdot \|\|_2$	=	l_2 norm
SNR	=	Signal to Noise Ratio